

High-Throughput Craniofacial Development Phenotyping in Zebrafish using VAST BioImager

Work performed at the Center for Human Disease Modelling, Duke University by Zachary Kupchinsky, Erica Davis and Nicolas Katsanis

Technical note was prepared by Mikalai Malinouski, Union Biometrica, Holliston, MA

Zebrafish is an emerging vertebrate model organism to study human diseases and toxicology [1]. A variety of genetic tools in zebrafish allow *in vivo* modeling of human genetic diseases and regeneration [2]. Zebrafish larvae also have small size and optical clarity which allows easy microscopic evaluation of physiological changes and morphological phenotypes. Conventional imaging approaches involve manual orientation of each larva and are difficult to automate for genetic and drug screens. Here we report how VAST Biolmager [3] was used to automate zebrafish larvae positioning, orientation and image collection for a large numbers of zebrafish larvae. Mutations in mapre2 gene lead to defects in normal craniofacial development in zebrafish larvae [4]. Mutations in human MAPRE2 are linked to circumferential skin creases Kunze type ("Michelin tire baby") [5]. MAPRE2 encodes a member of tubulin binding family and is thought to control microtubule dynamics and reorganization [6].

Method

Heterozygous zebrafish 1.4col1a1:egfp were outcrossed with AB strain adults. Zebrafish embryos were injected with 1 nL (6ng morpholino and/or 100pg of human MAPRE2 mRNA) at the 1-4 cell developmental stage. 50-100 embryos were injected for each experimental condition. Embryos were then maintained at 28° C in E3 media (0.3 g/L NaCl, 75 mg/L CaSO₄, 37.5mg/L NaHC0₃, 0.003% methylene blue). 2-4 days post-fertilization (dpf) zebrafish larvae were anesthetized with 0.2 mg/ml tricaine and loaded using VAST Biolmager for collection of images (Fig. 1) [7][8].

Dorsal and lateral imaging templates were created each day to facilitate precise rotational orientation. The minimum similarity was set at 0.7. Fluorescence images of ventral view in the head area were collected in a fully automated way using Zeiss Axioscope A1 microscope, 5x Fluar objective, and Axiocam 503 camera. Zen Pro (Zeiss) imaging software was integrated to automatically collect images when directed by VAST Biolmager. GFP was excited with 470nm LED module.



Figure 1. VAST BioImager mounted on high-resolution compound microscope for automated positioning and imaging of zebrafish larvae.

Results

Morpholino suppression of mapre2 in zebrafish larvae resulted in craniofacial development phenotypes (Fig. 2A). First, fish injected with morpholinos had significantly increased the angle of the ceratohyal cartilage in 2-4 dpf larvae (Fig. 2B). In addition, test fish had a delay in the formation of ceratobranchial (cb) arch patterning. Most of the control 3dpf fish had three cb arches while less than 10% of morpholino injected fish showed this phenotype (Fig. 2C).

The similar pathophysiological phenotype was consistently observed using different morpholinos designed to mapre2. This craniofacial model was further tested to assess if complementation with human mapre2 mRNA will reverse the phenotype. Cb-directed arch formation in 3dpf was reversed to almost normal morphological levels. Furthermore, fish tested with mutated mapre2 mRNAs (missense mutations occurring in individual patients) was significantly worse than complementation with wild-type human MAPRE2.

Conclusions

VAST BioImager allowed for the development of a method and testing of a model for high-throughput phenotypic characterization of zebrafish larvae.

Acknowledgments

We thank Zachary Kupchinsky, Erica Davis and Nicolas Katsanis for developing the method and testing the samples.

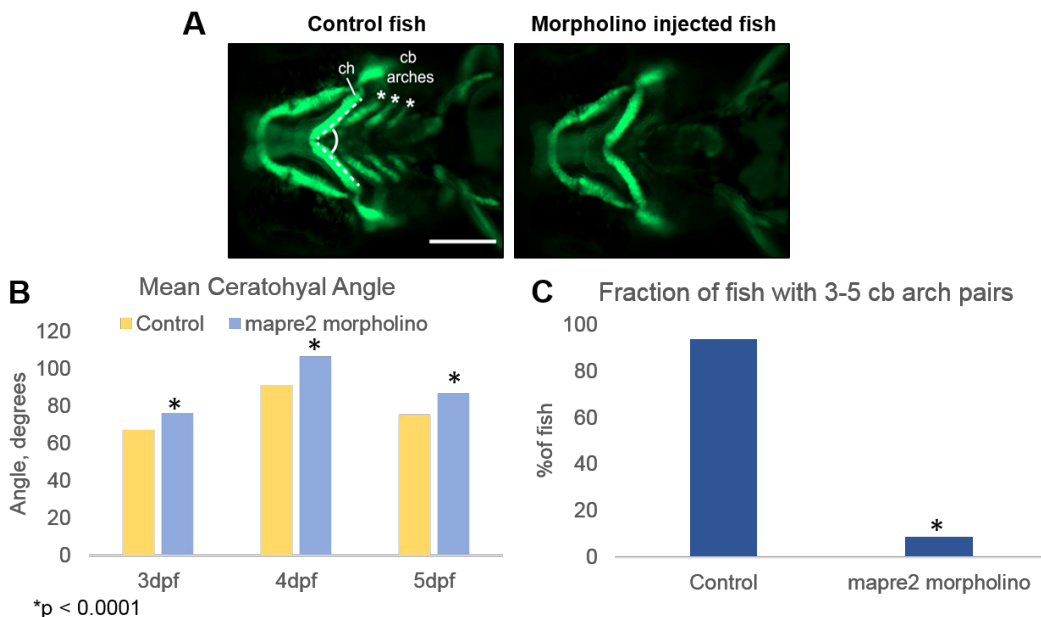


Figure 2. Automated analysis of zebrafish larvae using VAST Biolmager. Fish injected with mapre2 morpholinos demonstrate changes in craniofacial development. A. Phenotype of fish injected with mapre2 morpholinos was quantified using ceratohyal (ch) angle and fraction of fish with 3-5 ceratobranchial (cb) arches. Scale bar, 200 μ m. B. Cb angle measured using high-resolution fluorescence images of fish positioned with VAST Biolmager. Each bar graph represents mean of 20-48 larvae. C. Fraction of zebrafish larvae with 3-5 cb arches. Mapre2 depleted fish had delay in cb arches formation compare to wt control. Images of 36-48 fish were collected for each condition using VAST Biolmager automation and Zeiss compound microscope. Figure is adapted from [4].

References

- [1] K. Dooley and L. I. Zon, "Zebrafish: a model system for the study of human disease," *Curr. Opin. Genet. Dev.*, vol. 10, no. 3, pp. 252-256, Jun. 2000.
- [2] B. Goldstein and N. King, "The Future of Cell Biology: Emerging Model Organisms," *Trends Cell Biol.*, vol. 26, no. 11, pp. 818-824, Nov. 2016.
- [3] T.-Y. Chang, C. Pardo-Martin, A. Allalou, C. Wählby, and M. F. Yanik, "Fully automated cellular-resolution vertebrate screening platform with parallel animal processing," *Lab. Chip*, vol. 12, no. 4, pp. 711-716, Feb. 2012.
- [4] M. Isrie et al., "Mutations in Either TUBB or MAPRE2 Cause Circumferential Skin Creases Kunze Type," *Am. J. Hum. Genet.*, vol. 97, no. 6, pp. 790-800, Dec. 2015.
- [5] C. M. Ross, "Generalized Folded Skin With an Underlying Lipomatous Nevus: The Michelin Tire Baby," *Arch. Dermatol.*, vol. 100, no. 3, p. 320, Sep. 1969.
- [6] D. A. Goldspink et al., "The microtubule end-binding protein EB2 is a central regulator of microtubule reorganisation in apico-basal epithelial differentiation," *J. Cell Sci.*, vol. 126, no. Pt 17, pp. 4000-4014, Sep. 2013.
- [7] C. Pardo-Martin, T.-Y. Chang, B. K. Koo, C. L. Gilleland, S. C. Wasserman, and M. F. Yanik, "High-throughput *in vivo* vertebrate screening," *Nat. Methods*, vol. 7, no. 8, pp. 634-636, Aug. 2010
- [8] R. Pulak, "Tools for automating the imaging of zebrafish larvae," *Methods*, 96, pp. 118-126, 2016.